Synthesis and Characterization of Porphyrin-Sugar Carbon Conjugates[1]

Giovanni Casiraghi,*,† Mara Cornia,*,‡ Franca Zanardi,† Gloria Rassu,§ Enzio Ragg,⊥ and Rita Bortolini⊥

Dipartimento Farmaceutico dell'Università, Viale delle Scienze, I-43100 Parma, Italy, Dipartimento di Chimica Organica ed Industriale dell'Università, Viale delle Scienze, I-43100 Parma, Italy, Istituto per l'Applicazione delle Tecniche Chimiche Avanzate del CNR, Via Vienna 2, I-07100 Sassari, Italy, and Dipartimento di Scienze Molecolari Agroalimentari dell'Università, Via Celoria 2, I-20133 Milano, Italy

Received October 28, 1993•

The synthesis, structures, and spectroscopic properties of some 5,15-di-*C*-glycosyl-10,20-diarylporphyrins, representatives of a novel class of meso-*C*-glycoconjugated porphyrins, have been investigated. Porphyrins **9–14** were prepared in 6–16% yield by condensation of suitable dipyrrylglycosides with aryl aldehydes in the presence of either trifluoroacetic acid or BF_3 promoters. In all instances, α,β-configured porphyrins were preferentially formed, α,α isomers being only marginal products. The UV–vis spectra in $CHCl_3$ solution showed Soret bands which are red-shifted by about 20 nm as compared to the corresponding absorption maximum of the planar reference compound *meso*-5,15-bis(*p*-fluorophenyl)-10,20-diethylporphyrin (**15**). This suggested that the porphyrin macrocycles of **9-14** are inherently distorted to a significant extent. Detailed 1D and 2D ^1H NMR spectroscopic studies, including variable-temperature experiments in deuterated chloroform or tetrachloroethane, were carried out using the trans-disposed porphyrins **9** and **10**. It was found that, at ambient temperature, these porphyrins adopted distorted saddle conformations in solution. Molecular mechanics techniques were used to analyze the distortion of porphyrin **9** as determined by the orientation of carbohydrate legs on the porphyrin periphery.

Introduction

Porphyrinyl conjugates are ubiquitous in nature and biology.[2] They play pivotal roles in a variety of fundamental processes ranging from the oxygen binding to hemoglobin and myoglobin[3] to oxidations catalyzed by cytochrome P-450 enzymes[4] and bacterial photosynthesis.[5] As a result, increasing effort has been recently devoted to the design, synthesis, and exploitation of highly structured artificial porphyrins to mimic the properties of heme-containing enzymes. As an example, modeling the oxygen-transfer reaction of cytochrome P-450,[6] a number of chiral nonracemic (porphyrinato)metal(III) compounds have been designed and exploited in the catalytic asymmetric hydroxylation, epoxidation, and sulfoxidation domains.[7] In addition, conjugation of the porphyrin core with suitable recognition units has allowed construction of effective polytopic assemblies to be employed as artificial receptors,[8] molecular recognition devices,[9] carriers for the selective transport of biomolecules,[10] DNA binders,[11] and antiviral and anticancer chemotherapeutics.[12]

In this context, porphyrins with appended sugar tentacles should be of special importance since they conjugate in one molecule the intrinsic chirality and hydrophilicity

† Dipartimento Farmaceutico, Parma.
‡ Dipartimento di Chimica Organica ed Industriale, Parma.
§ Istituto CNR, Sassari.
⊥ Dipartimento di Scienze Molecolari Agroalimentari, Milano.

• Abstract published in *Advance ACS Abstracts,* March 1, 1994.

(1) *C*-Glycosylated Porphyrins. 2. For part 1, see: Cornia, M.; Casiraghi, G.; Binacchi, S.; Zanardi, F.; Rassu, G. *J. Org. Chem.*, in press. Taken in part from the Laurea Thesis of F.Z., University of Parma, 1991–1992. Preliminary communication of part of this work: Casiraghi, G.; Cornia, M.; Rassu, G.; Del Sante, C.; Spanu, P. *Nat. Prod. Lett.* **1992**, *1*, 45. See also: Casiraghi, G.; Cornia, M.; Rassu, G.; Del Sante, C.; Spanu, P. *Tetrahedron* **1992**, *48*, 5619. Rassu, G.; Casiraghi, G.; Spanu, P.; Pinna, L.; Cornia, M. XVIth International Carbohydrate Symposium; Paris, France, July 5–10, 1992; Abstracts p 587.

(2) Morgan, B.; Dolphin, D. *Structure and Bonding 64*; Buchler, J. W., Ed.; Springer-Verlag: Berlin, 1987.

(3) Perutz, M. F.; Fermi, G.; Luisi, B.; Shaanan, B.; Liddington, R. C. *Acc. Chem. Res.* **1987**, *20*, 309.

(4) Weber, L.; Haufe, G. *Z. Chem.* **1989**, *29*, 88.

(5) Boxer, S. G. *Biophys. Biochim. Acta* **1983**, *726*, 265.

(6) McMurry, T. J.; Groves, J. T. In *Cytochrome P-450: Structure, Mechanism and Biochemistry*; Ortiz de Montellano, P. R., Ed.; Plenum: New York, 1986; pp 1–28. Akhtar, M.; Wright, J. N. *Nat. Prod. Rep.* **1991**, *8*, 527. Mansuy, D.; Battioni, P.; Battioni, J. P. *Eur. J. Biochem.* **1989**, *184*, 267.

(7) O'Malley, S.; Kodadek, T. *J. Am. Chem. Soc.* **1989**, *111*, 9116. Groves, J. T.; Viski, P. *J. Org. Chem.* **1990**, *55*, 3628. Naruta, Y.; Ishihara, N.; Tani, F.; Maruyama, K. *Chem. Lett.* **1991**, 1933. Naruta, Y.; Tani, F.; Maruyama, K. *Tetrahedron: Asymmetry* **1991**, *2*, 533. Naruta, Y.; Tani, F.; Ishihara, N.; Maruyama, K. *J. Am. Chem. Soc.* **1991**, *113*, 6865. Halterman, R. L.; Jan, S. T. *J. Org. Chem.* **1991**, *56*, 5253. Maillard, P.; Guerquin-Kern, J. L.; Momenteau, M. *Tetrahedron Lett.* **1991**, *32*, 4901. Schurig, V.; Betschinger, F. *Chem. Rev.* **1992**, *92*, 873. Weber, L.; Imiolczyk, I.; Haufe, G.; Rehorek, D.; Henning, H. *J. Chem. Soc., Chem. Commun.* **1992**, 301. Collman, J. P.; Zhang, X.; Lee, V. J.; Brauman, J. I. *J. Chem. Soc., Chem. Commun.* **1992**, 1647. Chiang, L.; Konishi, K.; Aida, T.; Inoue, S. *J. Chem. Soc., Chem. Commun.* **1992**, 254. Konishi, K.; Oda, K.; Nishida, K.; Aida, T.; Inoue, S. *J. Am. Chem. Soc.* **1992**, *114*, 1313. Naruta, Y.; Tani, F.; Maruyama, K. *Tetrahedron Lett.* **1992**, *33*, 6323. Naruta, Y.; Ishihara, N.; Tani, F.; Maruyama, K. *Bull. Chem. Soc. Jpn.* **1993**, *66*, 158.

(8) Bonar-Law, R. P.; Sanders, J. K. M. *J. Chem. Soc., Chem. Commun.* **1991**, 574. Mihara, H.; Nishino, N.; Hasegawa, R.; Fijimoto, T. *Chem. Lett.* **1992**, 1805. Gunter, M. J.; Johnston, M. R. *Tetrahedron Lett.* **1992**, *33*, 1771. Imai, H.; Nakagawa, S.; Kyuno, E. *J. Am. Chem. Soc.* **1992**, *114*, 6719.

(9) Sessler, J. L.; Magda, D. In *Inclusion Phenomena and Molecular Recognition*; J. Atwood: New York, 1990; pp 17–26. Le Maux, P.; Bahri, H.; Simmoneaux, G. *J. Chem. Soc., Chem. Commun.* **1991**, 1350. Ogoshi, H.; Hatekeyama, H.; Kotani, J.; Kawashima, A.; Kuroda, Y. *J. Am. Chem. Soc.* **1991**, *113*, 8181. Mizutani, T.; Ema, T.; Tomita, T.; Kuroda, Y.; Ogoshi, H. *J. Chem. Soc., Chem. Commun.* **1993**, 520.

(10) Furuta, H.; Cyr, M. J.; Sessler, J. L. *J. Am. Chem. Soc.* **1991**, *113*, 6677. Kràl, V.; Sessler, J. L.; Furuta, H. *J. Am. Chem. Soc.* **1992**, *114*, 8704.

(11) Fiel, R. J. *J. Biomol. Struct. Dynam.* **1989**, *6*, 1259. Ding, L.; Etemad-Moghadam, G.; Cros, S.; Auclair, C.; Meunier, B. *J. Med. Chem.* **1991**, *34*, 900. Marzilli, L. G.; Petho, G.; Lin, M.; Kim, M. S.; Dixon, D. W. *J. Am. Chem. Soc.* **1992**, *114*, 7575.

(12) Pandey, R. K.; Shiau, F. Y.; Ramachandran, K.; Dougherty, T. J.; Smith, K. M. *J. Chem. Soc., Perkin Trans. 1* **1992**, 1377. Adams, K. R.; Berenbaum, M. C.; Bonnett, R.; Nizhnik, A. N.; Salgado, A.; Vallés, M. A. *J. Chem. Soc., Perkin Trans. 1* **1992**, 1465. Woodburn, K. W.; Vardaxis, N. J.; Hill, J. S.; Kaye, A. H.; Reiss, J. A.; Phillips, D. R. *Photochem. Photobiol.* **1992**, *55*, 697.

0022-3263/94/1959-1801$04.50/0

Chart 1

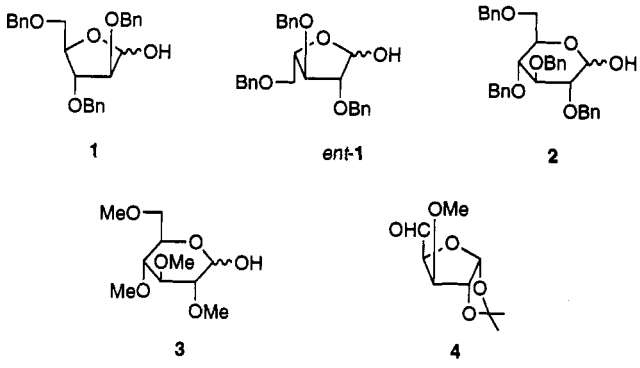

Chart 2

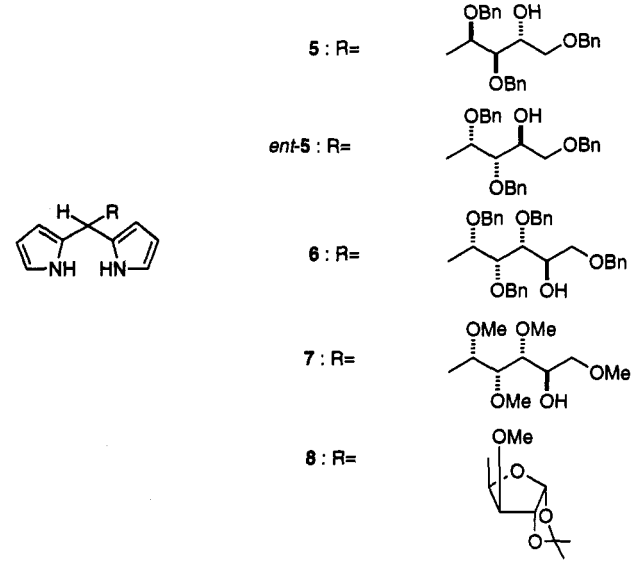

of the carbohydrate with the binding properties of the hydrophobic porphyrin cavity. While there are now a number of studies dealing with the synthesis and use of porphyrins bonded to a carbohydrate by heteroatom-involving linkages,[13] only marginal attention has been paid to preparation of porphyrin–sugar carbon–carbon conjugates.[14,15] We describe here a conceptually simple entry to a novel class of glycoporphyrins where the sugar moieties are anchored to the meso carbon of the macrocycle by means of chemically and metabolically robust carbon–carbon bonds.[16] We also wish to report their characterization as well as a molecular mechanics study.

Results and Discussion

Synthesis of 5,15-Bis-Glycosylated Porphyrins. Among the various means by which a porphyrin ring can be constructed, the acid-catalyzed condensation of dipyrrylmethane units with aryl aldehydes represents a widely exploited route. We have used this technique to arrive at meso bis-glycosylated diarylporphyrins in this study. This approach took advantage of the accessibility of homochiral dinuclear *C*-glycosyl subunits by a protocol involving direct condensation of aldoses with pyrrole. Thus, condensation of furanosyl and pyranosyl aldoses **1-4** in Chart 1 with pyrrole (1:5 molar ratio) was effected in methylene chloride at room temperature in the presence of 1.0 equiv of $SnCl_4$. The reaction was complete within 1 h, and after aqueous $NaHCO_3$ quenching and flash chromatographic purification, the dipyrrylmethanes **5-8** listed in Chart 2 were obtained in 30–40% isolated yields. As expected, the ^1H and ^{13}C NMR spectra of these substances displayed distinct resonances for all the pyrrole methyne protons and carbons, owing to diastereotopicity of the two pyrrole units appended at the homochiral sugar fragment.

With significant quantities of **5–8** in hand, we next turned to macrocycle construction. The condensation of the bipyrrole subunits with 4-fluorobenzaldehyde (PFBA) or benzaldehyde (BA) was performed according to the procedures developed by Anderson,[17] Gunter,[18] and others.[19] Here, the porphyrin-forming reaction was carried out in dry CH_2Cl_2 in the dark and under high-purity argon atmosphere in the presence of either trifluoroacetic acid (TFA) or BF_3 etherate. Following oxidation of the porphyrinogen intermediates by DDQ and flash chromatographic separation on silica gel, porphyrins **9–14** listed in Chart 3 were obtained in yields ranging from 6% to 16%. Table 1 summarizes the synthetic results.

For robust benzyl- and methyl-protected derivatives, TFA was the catalyst of choice, while BF_3 etherate served with both acid-sensitive and resistant compounds. However, while in all instances the TFA-based procedure gave rise to a single porphyrin isomer, the use of BF_3 etherate sometimes produced mixtures of two isomeric compounds.[20] That stereoisomers **9–13** indeed possess the trans (α,β) configuration and **14** the cis (α,α) configuration as shown in Chart 3 was only tentative at this point, assuming that the predominant isomers in these ring-forming reactions would be the more stable ones and that the more stable isomers would have the two carbohydrate legs in a transoid α,β location (vide infra).

Characterization of the Glycoporphyrins. The porphyrinyl conjugates **9–14** were subjected to various spectral analyses, including mass, UV–vis absorption, circular dichroism (CD), and ^1H NMR spectroscopies. All the compounds are homogeneous and virtually pure materials; this was ascertained by reversed-phase HPLC analyses on a μ-Bondapack C-18 column eluting with methanol–water solvent mixtures. In addition, when heated in toluene at 110 °C for several days under an argon atmosphere, they proved to be stable toward atropoisomerization. Low-resolution chemical ionization

(13) Maillard, P.; Guerquin-Kern, J. L.; Momenteau, M.; Gaspard, S. *J. Am. Chem. Soc.* **1989**, *111*, 9125. Fülling, G.; Schröder, D.; Franck, B. *Angew. Chem., Int. Ed. Engl.* **1989**, *28*, 1519. Kohata, K.; Yamaguchi, Y.; Higashio, H.; Odashima, T.; Ishii, H. *Chem. Lett.* **1992**, 477. Fuhrhop, J. H.; Demoulin, C.; Boettcher, C.; Koning, J.; Siggel, U. *J. Am. Chem. Soc.* **1992**, *114*, 4159. Weber, L.; Imiolczyk, I.; Haufe, G.; Rehorek, D.; Hennig, H. *J. Chem. Soc., Chem. Commun.* **1992**, 301.

(14) Ono, N.; Bougauchi, M.; Maruyama, K. *Tetrahedron Lett.* **1992**, *33*, 1629.

(15) Recently, an unusual modified porphyrinyl *C*-glycoside (tolyporphyn) bearing two dideoxyxylohexopyranose units β-linked to C-7 and C-17 was isolated from the blue-green alga *Tolypotryx nodosa*. Prinsep, M. R.; Caplan, F. R.; Moore, R. E.; Patterson, G. M. L.; Smith, C. D. *J. Am. Chem. Soc.* **1992**, *114*, 385.

(16) Since this work was completed, a paper dealing with the synthesis of *meso*-tetrakis(glycosylated)porphyrins had appeared: Maillard, P.; Huel, C.; Momenteau, M. *Tetrahedron Lett.* **1992**, *33*, 8081. We thank Prof. P. Maillard for communicating his results prior to publication.

(17) Anderson, H. L.; Sanders, J. K. M. *J. Chem. Soc., Chem. Commun.* **1989**, 1714. Anderson, H. *Tetrahedron Lett.* **1992**, *33*, 1101.

(18) Gunter, M. J.; Mander, L. N. *J. Org. Chem.* **1981**, *46*, 4792.

(19) Manka, J. S.; Laurence, D. S. *Tetrahedron Lett.* **1989**, *30*, 6989. Osuka, A.; Nagata, T.; Kobayashi, F.; Murayama, K. *J. Heterocycl. Chem.* **1990**, *27*, 1657. Lecas-Nawrocka, A.; Boitrel, B.; Rose, E. *Tetrahedron Lett.* **1992**, *33*, 481.

(20) Due to hindered rotation of the sugar residues in the meso positions of the macrocycle, two atropoisomeric compounds are in principle possible. Here, they are termed cis (α,α) and trans (α,β), respectively. See also ref 2.

Chart 3

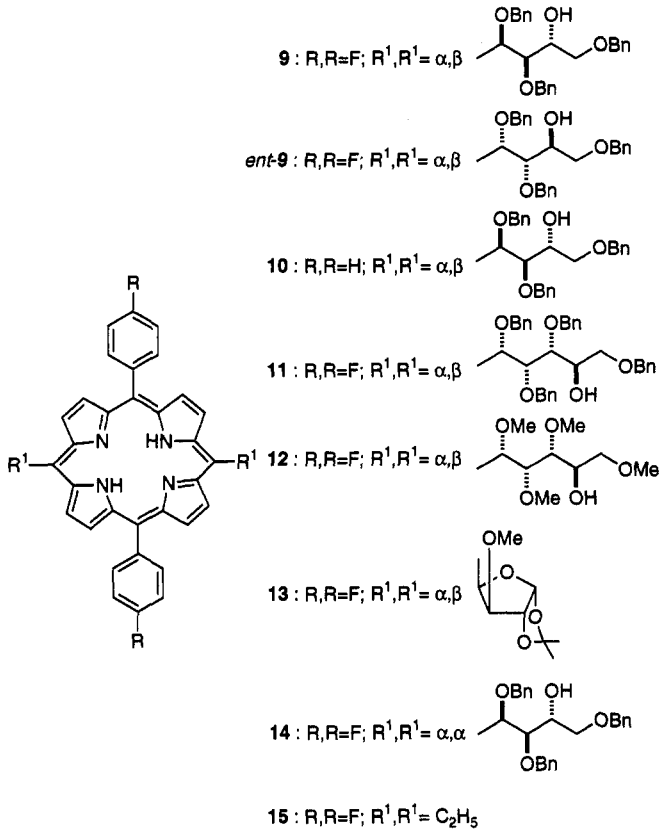

Table 1. Synthesis of Porphyrins 9–14[a]

products	dipyrrylmethane precursor	aldehyde	promoter	% isolated yield
9	5	PFBA	TFA	6.0
ent-9	*ent*-5	PFBA	TFA	8.4
9 + 14	5	PFBA	BF_3	6.0 + 4.0
10	5	BA	TFA	7.2
11	6	PFBA	TFA	16
12	7	PFBA	TFA	7.2
13	8	PFBA	BF_3	3.6
15	DPP	PFBA	TFA	16

[a] Key: PFBA = 4-fluorobenzaldehyde; BA = benzaldehyde; DPP = 1,1-dipyrrylpropane; TFA = trifluoroacetic acid.

(CH_4) mass spectra gave molecular weights which are those expected of the corresponding $(M + H)^+$ formulas, while high-resolution MS gave the corresponding exact mass measurements.

In the UV–vis spectra, the Soret bands at 413–421 nm and four Q bands at ca. 515, 550, 590, and 650 nm showed the presence of a porphyrin ring (Table 2).

The Soret bands were significantly red-shifted compared to the reference porphyrin 5,15-bis(4-fluorophenyl)-10,-20-diethylporphyrin (**15**) (401 nm; $\epsilon = 49.0 \times 10^3$) with reduced ϵ values. In the Q-band region, similar spectra were obtained for trans-configured α,β porphyrins **9–13**, showing typical patterns of four maxima with decreasing intensity. On the contrary, cis-configured α,α isomer **14** displayed an unusually intense band at 653 nm ($\epsilon = 3.7 \times 10^3$). Several studies have investigated the effects of nonplanarity of the porphyrin macrocycle on the visible absorption spectra of congested derivatives.[21] The studies have shown that the absorption maxima of nonplanar porphyrins are shifted at lower energy (red) when compared to planar counterparts. As shown in Table 2, both the Soret bands and Q bands in glycoporphyrins **9–14** are significantly shifted to lower energy compared to the planar prototype **15**; this suggested that, in chloroform solution, these porphyrins indeed might adopt distorted nonplanar structures. Accordingly, a nonplanar conformation was obtained as a minimum energy structure for **9** using a molecular mechanics force field, which showed that the observed conformation was due to steric repulsions between the pyrrole rings and the peripheral phenyl and sugar moieties (vide infra).

Table 2. UV-vis Data for Porphyrins 9–14[a]

porphyrin	Soret	Q_1	Q_2	Q_3	Q_4	concn ($M \times 10^{-3}$)
9	419 (29.7)	516 (2.0)	547 (0.9)	590 (0.6)	646 (0.4)	0.13
ent-9	418 (34.7)	517 (2.2)	549 (0.8)	590 (0.7)	646 (0.4)	0.13
10	414 (85.9)	517 (8.7)	551 (3.1)	591 (2.7)	646 (2.0)	0.045
11	417 (37.9)	515 (3.3)	549 (1.3)	589 (1.2)	645 (0.7)	0.10
12	413 (31.9)	514 (3.1)	547 (0.9)	589 (1.0)	643 (0.4)	0.12
13	421 (13.3)	517 (0.6)	553 (0.5)	591 (0.3)	645 (0.2)	0.14
14	417 (27.4)	518 (2.3)	547 (1.4)	598 (0.8)	653 (3.7)	0.14
15	401 (49.0)	502 (8.1)	535 (2.8)	576 (2.8)	630 (1.0)	0.09

[a] λ, nm ($\epsilon = 10^{-3}$ cm^{-1} M^{-1}).

The chloroform solutions of all porphyrinyl glycoconjugates **9–14** were optically and CD active. The two enantiomeric trans porphyrins **9** and *ent*-**9** showed clean CD-induced spectra in the range 350–680 nm that are mirror images of each other, with intense bands at 419 nm ($[\theta] = \pm 1.56 \times 10^4$ deg cm^2 $dmol^{-1}$) corresponding to the Soret absorptions in the electronic spectra. Two additional bands at 317 and 430 nm can also be seen, accompained by two small Q-bands of opposite signs at 516 and 556 nm. The cis isomer **14** showed a quite different CD profile, with a weak negative absorption centered at 417 nm ($[\theta] = -2.4 \times 10^3$ deg cm^2 $dmol^{-1}$) and a pronounced band at 653 nm which corresponds to the characteristic long-wavelength Q-band in the electronic spectrum. The reduced ellipticity of **14** compared to the corresponding isomer **9** may be attributed to the more crowded arrangement of the two alditol legs in **14** on the same side of the macrocycle which disturbs their overlap on the porphyrin core giving, as a result, weaker ellipticity.[22] The CD spectral profiles of **10** and **13** showed simple positive Cotton effects for the whole Soret band region, whereas D-glucose-based OMe and OBn derivatives **11** and **12** displayed similar but complex profiles involving, in the Soret region, alternate negative and positive bands. The fine structure of the CD is too complicated for resolution by the instrument employed.

^1H NMR spectroscopy was used to definitively identify the porphyrins of this study. The detailed assignments proved difficult due to the presence of several overlapped signals in the 1D spectra and required extensive use of 2D techniques including COSY, NOESY, and ROESY experiments. In general, the protons at the following positions are responsible for the signals in the indicated regions of the spectra: (a) pyrrole β,β'-protons between

(21) Medforth, C. J.; Smith, K. M. *Tetrahedron Lett.* **1990**, *31*, 5583. Hombrecher, H. K.; Horter, G.; Arp, C. *Tetrahedron* **1992**, *48*, 9451.

(22) Nishino, N.; Mihara, H.; Hasegawa, R.; Yanai, T.; Fujimoto,T. *J. Chem. Soc., Chem. Commun.* **1992**, 692.

Table 3. ^{1}H NMR Spectral Data for Porphyrins 9–15[a]

compd	pyrrole β-H	pyrrole β′-H	phenyl H_{ortho}	phenyl H_{meta}	H-1′	H-2′	OH	NH
9	10.35 (d), 10.28 (d), 9.38 (d), 9.36 (d)	8.78 (d), 8.74 (d), 8.69 (d)	8.21 (m), 8.13 (m), 8.04 (m)	7.42 (m)	7.39 (d), 7.38 (d)	3.88 (d), 3.85 (d)	2.67 (d), 2.60 (d)	−2.68 (bs)
10	10.29 (d), 10.23 (d), 9.36 (d), 9.32 (d)	8.79 (d), 8.77 (d), 8.75 (d), 8.71 (d)	8.22 (m), 8.14 (m)	7.62 (m)	7.42 (d), 7.38 (d)	4.57 (m)	2.65 (d), 2.58 (d)	−2.68 (bs)
11	10.18 (d), 10.15 (d), 9.43 (d), 9.41 (d)	8.75 (d), 8.72 (d), 8.56 (m)	7.98 (m)	7.38 (m)	7.49 (m), 7.25 (m)	5.19 (m), 4.69 (m)	2.95 (bs), 2.85 (bs)	−2.78 (bs)
12	10.03 (d), 9.99 (d), 9.76 (d), 9.72 (d)	8.91 (d), 8.87 (d), 8.83 (m)	8.27 (m), 8.13 (m), 7.99 (m)	7.47 (m)	7.16 (d)	5.08 (d), 5.00 (d)	3.00 (d), 2.22 (d)	−2.85 (bs)
13	9.62 (d), 8.81 (m)	8.73 (d), 7.83 (m)	8.10 (m)	7.38 (m)	6.63 (m)	4.25 (m)		−2.90 (bs)
14	10.04 (d), 9.84 (d), 9.79 (d), 9.03 (d)	8.49 (d), 8.41 (d), 8.34 (d), 8.09 (d)	7.90–7.60 (m)	7.40 (m)	7.30 (m), 6.30 (d)	4.72–4.50 (m), 4.28 (m)	2.62 (bs)	−1.00 (bs), −1.40 (bs)
15	9.32 (d)	9.11 (d)	8.22 (m)	7.50 (m)				−3.13 (bs)

[a] Chemical shifts (ppm) in $CDCl_3$ (multiplicity).

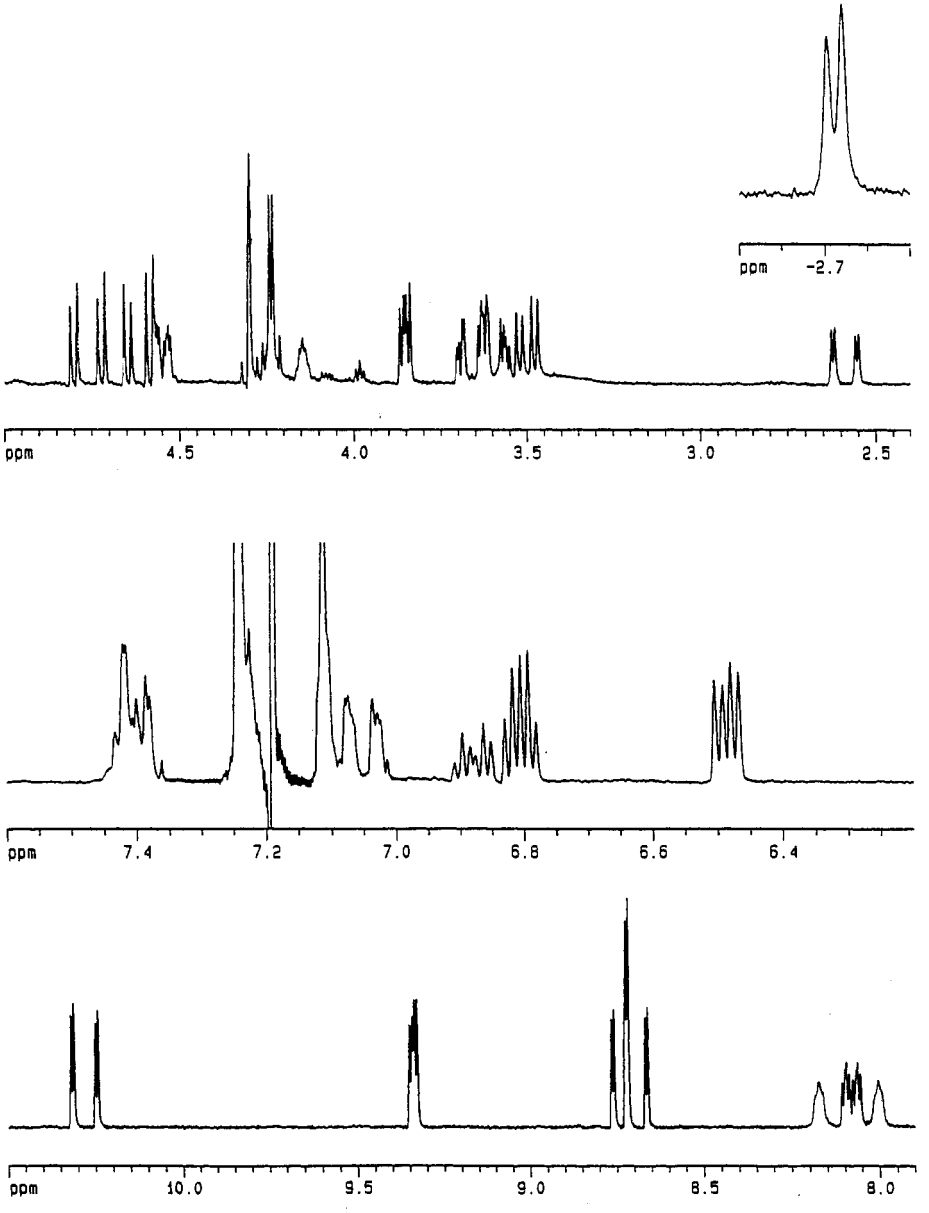

Figure 1. Expanded ^{1}H NMR spectrum of porphyrin 9 in $CDCl_3$ at 293 K taken at 600.1 MHz. The peak at 7.23 ppm is due to $CHCl_3$. For assignments, see Table 3.

10.5 and 8.5 ppm, (b) meso phenyls and other aromatics (8.5 to 7.0 ppm), (c) protons at C-1′ (7.5 to 6.5 ppm), (d) other protons of the sugar legs (5.0 to 3.0 ppm), (e) OHs (3.0 to 2.2 ppm), and (f) NHs (−1.0 to −2.9 ppm). A summary of selected proton assignments is reported in Table 3.

As an example, the 600 MHz NMR spectrum of **9** in deuterated $CHCl_3$ is shown in Figure 1 evidencing the diagnostic signals. In order to assign the pyrrole proton to β and β′ positions, use was made of the fact that NOE contacts were observed between β protons and H-1′ of the adjacent sugar mojeties, while β′ protons that flank the

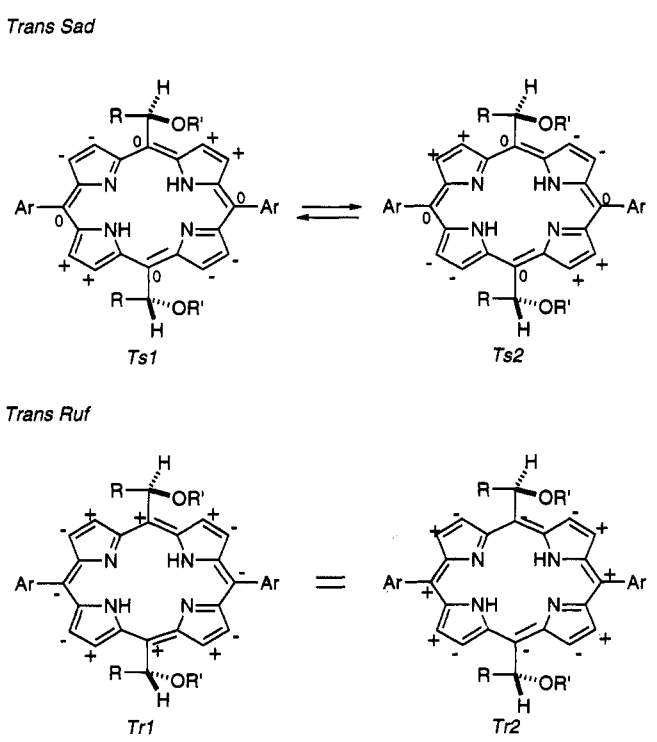

Figure 2. Idealized *sad* and *ruf* distorsion modes for the trans porphyrin macrocycle. Displacements of the atoms from the mean porphyrin plane are shown as + (above), − (below), and 0 (in plane).

meso aryl groups correlated solely with the aryl H_{ortho} protons. At room temperature (293 K), the spectrum of **9** shows eight doublets for the β,β' pyrrole protons, four slightly overlapped triplets for the ortho protons of the meso phenyls, two doublets for the protons at C-1′, two doublets for OHs, and two close singlets for NHs,[23] each signal integrating to one proton. If the tetrapyrrole macrocycle were planar or adopted a nonplanar conformation with rapid inversion, one would expect a spectrum with half signals each integrating to two protons, owing to the overall C_2 symmetry of the molecule which possesses an on-plane binary symmetry axis intersecting the meso aryls.

Recent solution- and solid-state studies have illustrated the flexibility and the distortions imposed on the porphyrinyl macrocycles by the presence of large peripheral substituents.[24] The distorsion of the macrocycle leads to two different conformations termed *sad* (saddle) and *ruf* (ruffled). In the *sad* form, each of the pairs of β pyrrole carbons are alternately placed above and below the porphyrin mean plane, while the four meso carbons are in the mean porphyrin plane. In the *ruf* form, the opposite pyrrole rings are counterrotated so that the meso carbons are alternately disposed above and below the mean porphyrin plane. Figure 2 shows a generalized picture of the expected *sad* and *ruf* forms of the porphyrins of this study, while the expected ^{1}H NMR spectral characteristics depending on the symmetry element present and the distorsion mode are summarized in Table 4.

Table 4. Symmetry Dependence of the Expected Proton Spectra for the *sad* and *ruf* Forms of Trans Porphyrins[a]

conformer	symmetry	group intersected by the axis	β,β'-pyrrole protons	phenyl H_{ortho}
Ts1	C_2	C(10)–C(20)	four doublets	two doublets
Ts2	C_2	C(10)–C(20)	four doublets	two doublets
Tr1=Tr2	C_1		eight doublets	four doublets

[a] Maximum number of expected signals for each type of proton. Ts and Tr refer to structures in Figure 2.

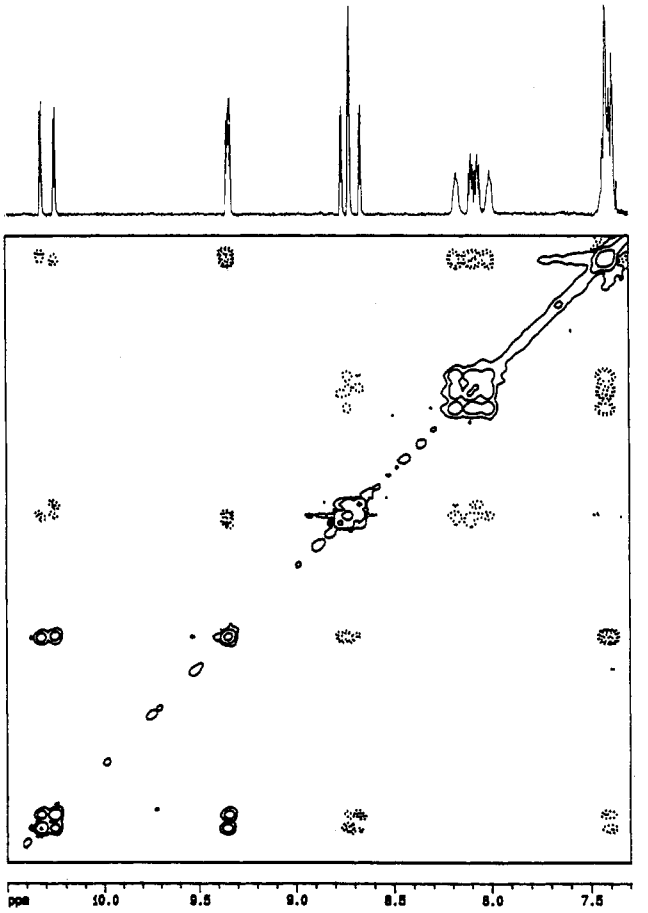

Figure 3. 2D ROESY expansion of the aromatic region for compound **9**, taken at 600.1 MHz in $CDCl_3$ with 300-ms spin lock. Contours arising from chemical exchange or through-space interactions are drawn in continuous or dotted lines, respectively.

From this analysis one must conclude that at 293 K porphyrin **9**, as well as the other closely related trans-configurated congeners **10**–**13**, exists either in a single dissymmetric trans-ruffled conformation or in a slowly interconverting 1:1 mixture of two C_2 symmetric nonplanar saddle conformations. In order to solve this dilemma, 2D ROESY experiments at 293 K were carried out. The ROESY spectra give information on the conformational flexibility of **9** in $CDCl_3$ solution. The experiment (Figure 3) allows the eight β,β' pyrrole proton resonances to be grouped into two sets of four and the four aromatic H_{ortho} signals into two sets of two. Each set corresponds to one of the chemically distinct types of pyrrole and phenyl ortho protons according to its own chemical environment. All the exchange cross-peaks, with the same sign as the diagonal, that correlate the protons, have the same intensity, indicating a rapid scrambling among the sites.

(23) In the expanded ^{1}H NMR spectrum of **9** (Figure 1), the two partially overlapped NH signals at ca. −2.7 ppm do not seem to have exactly the same intensity. This discrepancy may be due to instrumental difficulty in phasing the spectrum.

(24) (a) Hoard, J. L. In *Porphyrins and Metalloporphyrins*; Smith, K. M., Ed.; Esevier: Amsterdam, 1975; Chapter 8. (b) Barkigia, K. M.; Berber, M. D.; Fajer, J.; Medforth, C. J.; Renner, M. W.; Smith, K. M. *J. Am. Chem. Soc.* **1990**, *112*, 8851. (c) Medforth, C. J.; Senge, M. O.; Smith, K. M.; Sparks, L. D.; Shelnutt, J. A. *J. Am. Chem. Soc.* **1992**, *114*, 9859. (d) Munro, O. Q.; Bradley, J. C.; Hancock, R. D.; Marques, H. M.; Marsicano, F.; Wade, P. W. *J. Am. Chem. Soc.* **1992**, *114*, 7218.

Cross-relaxation cross-peaks with signs opposite to the diagonal can also be observed between the β and β' pyrrole protons, between β pyrrole and H-1′ and H-2′ protons, and between β' pyrrole and H_{ortho} protons. Taken together, the experimental results provide evidence of an exchange process involving two conformations, supporting the hypothesis that, at room temperature in $CDCl_3$ solution, **9** indeed consists of two equimolecular C_2 symmetric saddle conformations,[25] ruling out the alternative possibility that the porphyrin could have a totally dissymmetric ruffled nature.

Variable-temperature ^1H NMR spectroscopy has been extensively used to study nonplanar conformations of congested porphyrins and metalloporphyrins in solution.[24b,c] A similar investigation was performed on compound **10** which displayed well-resolved resonances for several diagnostic protons. In the more diagnostic region between 11.0 and 7.0 ppm the spectrum at 293 K [400 MHz, $(CDCl_2)_2$] shows eight doublets for the β,β' pyrrole protons, four doublets for the H_{ortho} of the meso phenyl groups, and two doublets for the protons at C-1′ of the carbohydrate legs. At 370 K the spectrum shows two broad resonances for the β pyrrole protons, a broad singlet for the β' protons, and two doublets assigned to H_{ortho} and H-1′ proton resonances, respectively. Unfortunately, the boiling point of the solvent and the instrumental limitations prevent the observation of the expected symmetric pattern of six well-resolved doublets. Coalescence occurs at ca. 338 K for the H_{ortho} doublet, at ca. 333 K for the β' pyrrole signal, and at ca. 328 K for the H-1′ doublet. The coalescence temperature, T_c, can be used to calculate the free energy of activation for different protons to become equivalent by using the standard equation, $\Delta G^*/RT = 22.96 + \ln(T_c/\delta\nu)$, where $\delta\nu$ is the difference in the respective ^1H resonances.[26] For the above coalescence temperatures, this equation yielded values of 16.6, 17.0, and 16.9 kcal mol^{-1}, respectively. By analogy with other congested nonplanar porphyrins,[24c] the dynamic process was assigned as the inversion of the saddle-shaped macrocycle as shown in Figure 4.

Molecular Mechanics Study. In order to gain some insight on the conformational properties of the glycoconjugated porphyrins of this study, molecular mechanics calculations on porphyrin **9** were performed. In agreement with the NMR data, the minimum energy structure was calculated to be a *sad* conformation (Figure 4).

Actually, it was possible to generate two structures of comparable energy by changing the relative displacements of the atoms in the porphyrin core. The inversion barrier between these two structures corresponds to the loss in energy when a saddle-shaped porphyrin is forced to adopt a planar conformation and was calculated to be approximately 15 kcal mol^{-1}. The saddle distorsion is generated from the steric repulsion that exists between pyrrole protons in the β-position and the chain substituents in 1′. This steric repulsion is responsible of the high energy barrier (about 30 kcal mol^{-1}) for the inversion process of the side chains (cis/trans equilibration). However, due to the high number of degrees of freedom of the benzylated carbohydrate chains, a more rigorous calculation should also take into account entropic contributions and thus calculate free energy, rather than total energy variations. Any attempt to generate a structure in a *ruf* conformation was unsuccessful because the energy minimization procedure always drove the geometry back to a *sad* conformation.

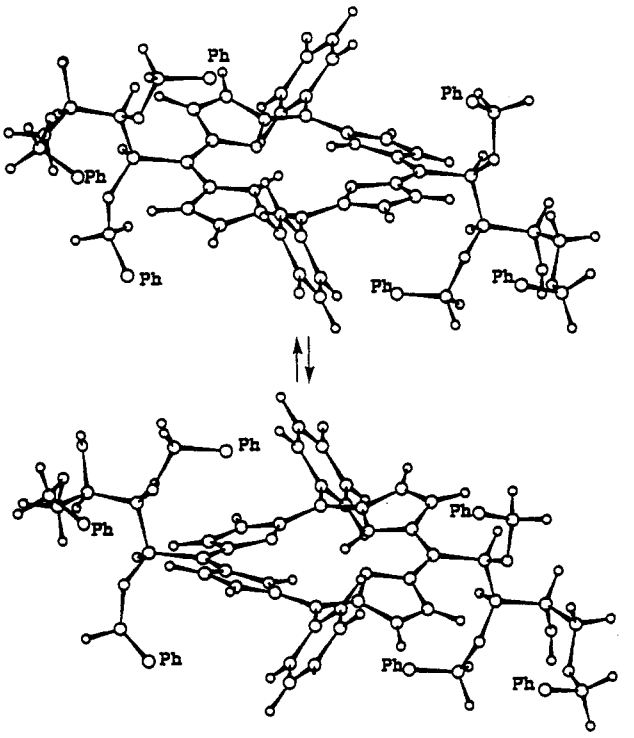

Figure 4. Representation of the macrocycle inversion process of the saddle structure of porphyrin **9**.

The derived structure possesses some similarities with the published X-ray data of the dodecaphenyl porphyrin, which was also found in a *sad* conformation.[24c] In that case, the distorsion from the nonplanarity of the porphyrin core was explained by the steric repulsions between the peripheral phenyl rings which remain tilted to minimize contacts. In our case, the phenyl groups are also found tilted, but the major source of steric repulsion resides on the carbohydrate chains.

Conclusions

We have been able to conceptualize, develop, and exploit a simple methodology for the synthesis of some *meso*-bis(*C*-glycosyl)diarylporphyrins **9–14**, representatives of a novel progeny of carbon–carbon-linked glycoconjugated porphyrins. We have investigated several aspects of the synthesis, structures, and spectroscopic properties of these conjugates. From the study, the following points emerge: (a) in the coupling procedure, α,β-configurational stereoisomers strongly predominate over the corresponding α,α-configurational counterparts; (b) for **9**, the observed ^1H NMR pattern is consistent with a nonplanar saddle conformation of the porphyrin macrocycle, with the ring inversion being slow on the NMR time scale at ambient temperature in $CDCl_3$ solution; (c) variable-temperature NMR studies and molecular mechanics calculations indicate that the dominant dynamic process for **9** (ΔG^* = 16.6–17.0 kcal mol^{-1}) is the inversion of the saddle-shaped

(25) Although a NH exchange process could in principle concur, we assumed that the predominant dynamic process was the inversion of the macrocycle. Accordingly, 2D ROESY NMR experiments on the dication of porphyrin **9** in $CDCl_3/CF_3CO_2H$ showed the presence of exchange cross-peaks between the β-pyrrole protons. We thank a reviewer for drawing this point to our attention.

(26) Abraham, R. J.; Fisher, J.; Loftus, P. In *Introduction to NMR Spectroscopy*; Wiley and Sons: Chichester, England, 1988.

porphyrin macrocycle. The demonstrated viability of the synthetic route herein paves the way for extension of the strategy to include Rothemund–Lindsey condensation between pyrrole and *aldehydo*-sugars[27] toward construction of novel amphiphilic symmetric and unsymmetric tetra-*C*-glycosylated porphyrin congeners. Further chemistry and uses of these porphyrins and their metalloderivatives are under investigation and will be the subject of future reports.[28]

Experimental Section

General Methods. All materials and solvents were obtained from commercial suppliers and were used without further purification. 2,3,5-Tri-*O*-benzyl-D-arabinofuranose (**1**), 2,3,5-tri-*O*-benzyl-L-arabinofuranose (*ent*-**1**), 2,3,4,6-tetra-*O*-benzyl-D-glucopyranose (**2**), and 2,3,4,6-tetra-*O*-methyl-D-glucopyranose were from Sigma; 1,2-*O*-isopropylidene-3-*O*-methyl-α-D-*xylo*-pentadialdofuranose (**4**) was from Fluka.

Flash chromatography was performed on 40–63 μm silica gel Merck no. 9385 or Florisil Carlo Erba 100–200 mesh, using the indicated solvent mixtures. Analytical thin-layer chromatography was performed on E. Merck silica gel 60 F_{254} plates (0.25 mm). The compounds were visualized by dipping the plates in a solution of Ce(III) sulfate (1.0 g), ammonium molybdate (21 g), 96% sulfuric acid (31 mL), and distilled water (500 mL). Emerald-green spots characterized all the porphyrins.

^{1}H NMR spectra were obtained on a Bruker AMX-400 or a Bruker AMX-600 and are reported in parts per millions (δ) relative to tetramethylsilane (0.0 ppm) as an internal reference, with coupling constants in hertz (Hz). Low-resolution mass spectra were obtained on a Finnigan 1020 6c mass spectrometer, and high-resolution mass spectra were obtained on a Kratos MS08RFA mass spectrometer. Rotations were measured on a Rudolph Autopol III polarimeter, while circular dichroism spectra were obtained on a JASCO 500 apparatus. Ultraviolet–visible spectra were obtained on a Kontron Uvicon 860 spectrophotometer.

Synthesis of Dipyrrylmethane Units. Typical Procedure: 2,3,5-Tri-*O*-benzyl-1,1-dipyrryl-1-deoxy-D-arabinitol (5). To a solution of pyrrole (0.35 mL, 50 mmol) and 2,3,5-tri-*O*-benzyl-D-arabinofuranose (**1**) in CH_2Cl_2 (35 mL) at ambient temperature with stirring under N_2 was added a solution of $SnCl_4$ (0.12 mL, 1 mmol) in CH_2Cl_2 (5 mL). After 60 min the bright orange reaction mixture was quenched by addition of a saturated aqueous $NaHCO_3$ solution (20 mL) and then with solid NH_4Cl (5 g). The resulting light yellow mixture was vigorously stirred for 15 min and extracted with diethyl ether (3 × 30 mL), and the combined extracts were dried ($MgSO_4$), filtered, evaporated, and purified by flash chromatography (7:3 hexane/EtOAc) to give 220 mg (40%) of **5** as a white solid: mp 146–148 °C; $[\alpha]^{20}_{546}$ +7.2°, $[\alpha]^{20}_{589}$ +7.5° (*c* 0.24, $CHCl_3$); ^{1}H NMR (400 MHz, $CDCl_3$) δ 8.72 (bs, 1H), 7.70 (bs, 1H), 7.40–7.00 (m, 15H), 6.61 (dd, *J* = 4.5, 2.5 Hz), 6.44 (dd, *J* = 4.4, 2.6 Hz), 6.07 (dd, *J* = 5.6, 2.5 Hz, 1H), 6.05 (dd, *J* = 5.5, 2.6 Hz), 5.96 (m, 1H), 5.90 (m, 1H), 4.49 (1/2 AB q, *J* = 10.3 Hz, 1H), 4.47–4.39 (m, 4H), 4.37 (d, *J* = 4.5 Hz, 1H), 4.16 (dd, *J* = 4.5 , 5.6 Hz, 1H), 4.04 (1/2 AB q, *J* = 10.3 Hz, 1H), 3.92 (m, 1H), 3.63 (dd, *J* = 5.6 , 9.5 Hz, 1H), 3.55–3.45 (m, 2H), 2.48 (bs, 1H); ^{13}C NMR (100 MHz, $CDCl_3$), CH_2 δ 75.3, 74.6, 73.6, 71.1, CH 130.0–127.0, 117.5, 116.4, 108.4, 108.0, 105.5, 83.8, 80.8, 70.7, 39.6, quaternary carbons 138.4, 138.2, 137.8, 131.6, 129.5; MS (CI, CH_4) *m/e* 537 (MH^+). Anal. Calcd for $C_{34}H_{36}N_2O_4$: C, 76.09; H, 6.76; N, 5.22. Found: C, 76.20; H, 6.95; N, 5.10.

The following compounds were obtained by adopting exactly this procedure.

2,3,5-Tri-*O*-benzyl-1,1-dipyrryl-1-deoxy-L-arabinitol (*ent*-5). This was prepared from *ent*-**1** in 42% yield: white solid; mp 145–147 °C; $[\alpha]^{20}_{589}$ −7.8° (*c* 0.22, $CHCl_3$); ^{1}H and ^{13}C NMR characteristics, see compound **5**; MS (CI, CH_4) *m/e* 537 (MH^+). Anal. Calcd for $C_{34}H_{36}N_2O_4$: C, 76.09; H, 6.76; N, 5.22. Found: C, 76.18; H, 6.85; N, 5.05.

2,3,4,6-Tetra-*O*-benzyl-1,1-dipyrryl-1-deoxy-D-glucitol (6). This compound was prepared from **2** in 30% yield: pale yellow oil; $[\alpha]^{20}_{589}$ +23.5° (*c* 0.20, $CHCl_3$); ^{1}H NMR (400 MHz, $CDCl_3$) δ 8.84 (bs, 1H), 7.66 (bs, 1H), 7.40–7.05 (m, 20H), 6.70 (m, 1H), 6.55 (m, 1H), 6.14 (dd, *J* = 6.2, 3.0 Hz, 1H), 6.13 (dd, *J* = 6.1, 3.1 Hz, 1H), 5.99 (m, 1H), 5.93 (m, 1H,), 4.72–4.45 (m, 7H), 4.33 (dd, *J* = 7.1, 3.1 Hz, 1H), 4.22 (d, *J* = 3.1 Hz, 1H), 4.16 (1/2 AB q, *J* = 10.5 Hz, 1H), 4.06 (m, 1H), 3.70–3.63 (m, 2H), 3.62–3.57 (m, 2H), 2.90 (bs, 1H); ^{13}C NMR (100 MHz, $CDCl_3$), CH_2 δ 75.8, 74.8, 73.5, 72.9, 71.3, CH 128.6–127.8, 117.7, 116.2, 108.6, 108.0, 105.3, 83.9, 80.0, 77.4, 70.7, 39.6, quaternary carbons 138.5, 138.0, 131.8, 128.8; MS (CI, CH_4) *m/e* 657 (MH^+). Anal. Calcd for $C_{42}H_{44}N_2O_5$: C, 76.80; H, 6.75; N, 4.26. Found: C, 76.92; H, 6.90; N, 4.15.

2,3,4,6-Tetra-*O*-methyl-1,1-dipyrryl-1-deoxy-D-glucitol (7). This compound was prepared from **3** in 33% yield: pale yellow oil; $[\alpha]^{20}_{546}$ −5.1°, $[\alpha]^{20}_{589}$ −4.1° (*c* 0.22, $CHCl_3$); ^{1}H NMR (400 MHz,$CDCl_3$) δ 8.96 (bs, m), 8.02 (bs, 1H), 6.75 (m, 1H), 6.65 (m, 1H), 6.17 (dd, *J* = 5.7, 3.0 Hz, 1H), 6.14 (dd, *J* = 5.7, 2.8 Hz, 1H), 6.07 (m, 2H), 4.32 (d, *J* = 3.4 Hz, 1H), 4.07 (dd, *J* = 7.5, 3.4 Hz, 1H), 3.92 (m, 1H), 3.80–3.20 (m, 16H), 2.87 (bs, 1H); ^{13}C NMR (100 MHz, $CDCl_3$), CH_3 δ 61.1, 60.7, 59.5, 59.1, CH_2 70.1, CH 117.7, 116.5, 108.5, 108.2, 107.9,104.7, 85.3, 82.7, 75.8, 73.5, 39.5, quaternary carbons 107.9, 107.7; MS (CI, CH_4) *m/e* 353 (MH^+). Anal. Calcd for $C_{18}H_{28}N_2O_5$: C, 61.34; H, 8.01; N, 7.95. Found: C, 61.30; H, 8.20; N, 7.80.

1,2-*O*-Isopropylidene-3-*O*-methyl-5,5-dipyrryl-5-deoxy-α-D-xylofuranose (8). This compound was prepared from dialdose **4** in 36% yield: pale yellow oil; $[\alpha]^{20}_{589}$ +10.4° (*c* 0.28, $CHCl_3$); ^{1}H NMR (400 MHz, $CDCl_3$) δ 8.94 (bs, 1H), 8.32 (bs, 1H), 6.69 (ddd, *J* = 2.6, 4.2, 6.8 Hz, 2H), 6.16 (dd, *J* = 2.6, 5.8 Hz, 1H), 6.10 (m, 1H), 6.08 (dd, *J* = 2.6, 5.8 Hz, 1H), 5.98 (d, *J* = 3.9 Hz, 1H), 5.82 (m, 1H), 4.52 (d, *J* = 3.9 Hz, 1H), 4.49 (d, *J* = 2.6 Hz, 1H), 4.47 (s, 1H), 3.36 (d, *J* = 2.6 Hz, 1H), 3.25 (s, 3H), 1.45 (s, 3H), 1.30 (s, 3H); ^{13}C NMR (100 MHz, $CDCl_3$), CH_3 δ 57.6, 26.8, 26.2, CH 117.2, 116.6, 108.2, 107.8, 107.0, 106.7, 105.4, 84.1, 83.4, 80.9, 39.0, quaternary carbons 132.1, 128.9, 111.8; MS (CI, CH_4) *m/e* 319 (MH^+). Anal. Calcd for $C_{17}H_{22}N_2O_4$: C, 64.13; H, 6.97; N, 8.80. Found: C, 64.00; H, 7.20; N, 8.65.

Synthesis of *C*-Glycosylporphyrins. Typical CF_3CO_2H-Promoted Condensation Procedure: 5,15-[Bis(4-fluorophenyl)]-10α,20β-[bis(1,2,4-tri-*O*-benzyl-D-*arabino*-tetritol-1-yl)]porphyrin (9). To a solution of dipyrrylmethane **5** (100 mg, 0.19 mmol) in 40 mL of CH_2Cl_2 were added sequentially 4-fluorobenzaldehyde (21 μL, 0.19 mmol) and trifluoroacetic acid (15 μL, 0.19 mmol) while a stream of pure argon was passing. The reaction vessel was carefully shielded from light, and stirring was continued for 3 h. Then, triethylamine (28 μL, 0.19 mmol) and dichlorodicyanobenzoquinone (DDQ) (90.8 mg, 0.4 mmol) were added, and the reaction mixture was stirred at room temperature for an additional 3 h. The solvent was evaporated under vacuum, and the resulting dark-violet solid dissolved in CH_2Cl_2 (2 mL). Florisil (1 g) was added and the solvent evaporated to give a powder which was charged at the top of a 20-mm i.d. silica gel column. Increasing polarity elution with 50:50 (v/v) CH_2Cl_2/hexane, 99:1 CH_2Cl_2/AcOEt, and 98:2 CH_2Cl_2/AcOEt gave rise to pure porphyrin **9** (7.6 mg, 6%) as a brown-red powder: R_f 0.58 (99.7:0.3 $CHCl_3$/MeOH); $[\alpha]^{20}_{546}$ −80°, $[\alpha]^{20}_{589}$ −43.6° (*c* 0.02, $CHCl_3$); UV–vis ($CHCl_3$) λ_{max} 419 nm (ε = 37850 cm^{-1} M^{-1}), 516 (ε = 1990), 547 (ε = 846), 590 (ε = 617), 646 (ε = 379); CD ($CHCl_3$) $[\theta]_{646}$ = −1193 deg cm^2 $dmol^{-1}$, $[\theta]_{590}$ = −746, $[\theta]_{547}$ = −490, $[\theta]_{516}$ = −980, $[\theta]_{419}$ = +15 592; ^{1}H NMR (600 MHz, $CDCl_3$) δ 10.35 (d, *J* = 4.9 Hz, 1H), 10.28 (d, *J* = 5.1 Hz, 1H), 9.38 (d, *J* = 4.9 Hz, 1H), 9.36 (d, *J* = 5.1 Hz, 1H), 8.78 (d, *J* = 4.9 Hz, 1H), 8.74 (m, 2H), 8.69 (d, *J* = 5.1 Hz, 1H), 8.21 (m, 1H,), 8.13 (m, 2H), 8.04 (m, 1H), 7.42 (m, 4H), 7.40–6.40 (m, 30H), 7.39 (d, *J* = 4.5 Hz, 1H), 7.38 (d, *J* = 4.3 Hz, 1H), 4.87–4.49 (m, 4H), 4.65 (m, 1H), 4.50 (m, 1H), 4.29 and 4.24 (2m, 4H), 4.21 (m, 1H), 4.17 (m, 1H), 3.82 (2 × 1/2 AB q, 2H), 3.66–3.44 (m, 4H), 3.45–3.38 (2 × 1/2 AB q, 2H), 2.67 (d, *J* = 5.8 Hz, 1H), 2.60 (d, *J* = 5.5 Hz,

(27) Rothemund, P.; Menotti, A. R. *J. Am. Chem. Soc.* **1941**, *63*, 267. Adler, A. D.; Longo, F. R.; Finarelli, J. D.; Goldmacher, J.; Assour, J.; Korsakoff, L. *J. Org. Chem.* **1967**, *32*, 476. Lindsey, J. S.; Schreiman, I. C.; Hsu, H. C.; Kearney, P. C.; Marguerettaz, A. M. *J. Org. Chem.* **1987**, *52*, 827.

(28) By using conventional chemistry, stable iron complex, **9**-$Fe^{III}Cl$, and manganese complex, **9**-$Mn^{III}Cl$, have been prepared in 70% and 72% yield, respectively. See: Adler, A. D.; Longo, F. R.; Kampas, F.; Kim, J. *J. Inorg. Nuc. Chem.* **1970**, *32*, 2443.

1H), -2.68 (bs, 2H); HRMS (CI, CH_4) exact mass calcd for $C_{82}H_{73}F_2N_4O_8$ 1279.5396 (MH^+), found 1279.5412. Anal. Calcd for $C_{82}H_{72}F_2N_4O_8$: C, 76.98; H, 5.67; N, 4.38. Found: C, 77.15; H, 5.90; N, 4.19.

The following porphyrins were obtained by adopting a quite similar procedure.

5,15-[Bis(4-fluorophenyl)]-10α,20β-[bis(1,2,4-tri-*O*-benzyl-L-*arabino*-tetritol-1-yl)]porphyrin (*ent*-9). From *ent*-5 and 4-fluorobenzaldehyde in 8.4% yield: red-brown powder; R_f 0.58 (99.7:0.3 $CHCl_3$/MeOH); $[\alpha]^{20}_{546}$ +85.6°, $[\alpha]^{20}_{589}$ +62.3° (*c* 0.01, $CHCl_3$); UV-vis ($CHCl_3$) λ_{max} 418 nm (ϵ = 34 650 cm^{-1} M^{-1}), 517 (ϵ = 2180), 549 (ϵ = 786), 590 (ϵ = 680), 646 (ϵ = 430); CD ($CHCl_3$) $[\theta]_{418}$ = +905 deg cm^2 $dmol^{-1}$, $[\theta]_{517}$ = -12, $[\theta]_{549}$ = -335, $[\theta]_{594}$ = -305, $[\theta]_{646}$ = -590; ^1H NMR, see compound **12**; HRMS (CI, CH_4) exact mass calcd for $C_{82}H_{73}F_2N_4O_8$ 1279.5396 (MH^+), found 1279.5420. Anal. Calcd for $C_{82}H_{72}F_2N_4O_8$: C, 76.98; H, 5.67; N, 4.38. Found: C, 76.80; H, 5.80; N, 4.50.

5,15-Diphenyl-10α,20β-[bis(1,2,4-tri-*O*-benzyl-D-*arabino*-tetritol-1-yl)]porphyrin (10). From **5** and benzaldehyde in 7.2% yield: red-brown powder; R_f 0.58 (99.7:0.3 $CHCl_3$/MeOH); $[\alpha]^{20}_{546}$ -68.4°, $[\alpha]^{20}_{589}$ +153.9° (*c* 0.006, $CHCl_3$); UV-vis ($CHCl_3$) λ_{max} 414 nm (ϵ = 85 900 cm^{-1} M^{-1}), 517 (ϵ = 8740), 551 (ϵ = 3090), 591 (ϵ = 2730), 646 (ϵ = 1960); CD ($CHCl_3$) $[\theta]_{414}$ = +74 990 deg cm^2 $dmol^{-1}$, $[\theta]_{517}$ = -104, $[\theta]_{551}$ = +1675, $[\theta]_{591}$ = +1040, $[\theta]_{646}$ = +2205; ^1H NMR (600 MHz, $CDCl_3$) δ 10.29 (d, *J* = 5.1 Hz, 1H), 10.23 (d, *J* = 4.9 Hz, 1H), 9.36 (d, *J* = 5.1 Hz, 1H), 9.32 (d, *J* = 4.9 Hz, 1H), 8.79 (d, *J* = 4.9 Hz, 1H), 8.77 (d, *J* = 5.1 Hz, 1H), 8.75 (d, *J* = 5.1 Hz, 1H), 8.71 (d, *J* = 4.9 Hz, 1H), 8.22 (m, 1H,), 8.14 (m, 2H), 8.07 (m, 1H), 7.62 (m, 6H), 7.42 (d, *J* = 3.3 Hz, 1H), 7.38 (d, *J* = 3.7 Hz, 1H), 7.35–6.45 (m, 30H), 4.85–4.55 (m, 4H), 4.57 (m, 2H), 4.28 and 4.23 (2m, 4H), 4.21 and 4.12 (2m, 2H,), 3.86 (2H, each 1/2 AB q), 3.75–3.52 (m, 4H), 3.57–3.45 (2H, each 1/2 AB q), 2.65 (m, 1H), 2.55 (m, 1H), -2.68 (bs, 2H); HRMS (CI, CH_4) exact mass calcd for $C_{82}H_{75}N_4O_8$ 1243.5585 (MH^+), found 1243.5604. Anal. Calcd for $C_{82}H_{74}N_4O_8$: C, 79.14; H, 6.07; N, 4.50. Found: C, 79.35; H, 6.30; N, 4.31.

5,15-[Bis(4-fluorophenyl)]-10α,20β-[bis(1,2,3,5-tetra-*O*-benzyl-D-*gluco*-pentitol-1-yl)]porphyrin (11). From **6** and 4-fluorobenzaldehyde in 16% yield: red-brown powder; R_f 0.63 (99.7:0.3 $CHCl_3$/MeOH); $[\alpha]^{20}_{546}$ +125.9°; $[\alpha]^{20}_{589}$ +118.2° (*c* 0.01, $CHCl_3$); UV-vis ($CHCl_3$) λ_{max} 417 nm (ϵ = 7850 cm^{-1} M^{-1}), 515 (ϵ = 3250), 549 (ϵ = 1275), 589 (ϵ = 1660), 645 (ϵ = 670); CD ($CHCl_3$) $[\theta]_{417}$ = -725 deg cm^2 $dmol^{-1}$, $[\theta]_{515}$ = +640, $[\theta]_{549}$ = -2280, $[\theta]_{589}$ = -145, $[\theta]_{645}$ = -775; ^1H NMR (600 MHz $CDCl_3$) δ 10.18 (d, *J* = 5.1 Hz, 1H), 10.15 (d, *J* = 4.9 Hz, 1H), 9.43 (d, *J* = 5.1 Hz, 1H), 9.41 (d, *J* = 4.9 Hz, 1H), 8.75 (d, *J* = 4.9 Hz, 1H), 8,72 (d, *J* = 5.1 Hz, 1H), 8.56 (m, 2H), 7.98 (m, 4H), 7.38 (m, 4H), 7.30–6.70 (m, 40H), 7.49 (m, 1H), 7.25 (m, 1H), 5.19 (m, 2H), 4.90–4.40 (m, 16H), 4.69 (m, 2H,), 3.96 (m, 1H), 3.57 (m, 4H), 3.33 (m, 1H), 2.95 (bs, 1H), 2.85 (bs, 1H), -2.78 (bs, 2H); HRMS (CI, CH_4) exact mass calcd for $C_{98}H_{89}F_2N_4O_{10}$ 1519.6546 (MH^+), found 1519.6563. Anal. Calcd for $C_{98}H_{88}F_2N_4O_{10}$: C, 77.45; H, 5.84; N, 3.96. Found: C, 77.71; H, 6.01; N, 3.77.

5,15-[Bis(4-fuorophenyl)]-10α,20β-[bis(1,2,3,5-tetra-*O*-methyl-D-*gluco*-pentitol-1-yl)]porphyrin (12). From **7** and 4-fluorobenzaldehyde in 7.2% yield: red-brown powder; R_f 0.17 (65.0:35.0 CH_2Cl_2/AcOEt); $[\alpha]^{20}_{546}$ +109.0°, $[\alpha]^{20}_{589}$ +54.5° (*c* 0.01, $CHCl_3$); UV-vis ($CHCl_3$) λ_{max} 413 nm (ϵ = 31 920 cm^{-1} M^{-1}), 514 (ϵ = 3140), 547 (ϵ = 930), 589 (ϵ = 985), 643 (ϵ = 390); CD ($CHCl_3$) $[\theta]_{413}$ = +1820 deg cm^2 $dmol^{-1}$, $[\theta]_{514}$ = +640, $[\theta]_{547}$ = -1110, $[\theta]_{589}$ = -166, $[\theta]_{643}$ = -910; ^1H NMR (600 MHz, $CDCl_3$) δ 10.03 (d, *J* = 5.1 Hz, 1H), 9.99 (d, *J* = 4.7 Hz, 1H), 9.76 (d, *J* = 4.9 Hz, 1H), 9.72 (d, *J* = 5.1 Hz, 1H), 8.91 (d, *J* = 4.9 Hz, 1H), 8.87 (d, *J* = 5.1 Hz, 1H), 8.83 (m, 2H), 8.27 (m, 1H,), 8.13 (m, 2H), 7.99 (m, 1H), 7.47 (m, 4H), 7.16 (d, *J* = 7.4 Hz, 2H), 5.08 and 5.00 (2d, *J* = 7.4 Hz, 2H), 3.98 (s, 6H), 3.74 (m, 2H), 3.62 (s, 3H), 3.55 (s, 3H), 3.41 (m, 1H), 3.21 (m, 5H), 3.00 (m, 1H), 2.95 and 2.94 (2s, 6H), 2.41 and 2.38 (2s, 6H), 2.22 (m, 1H), -2.85 (bs, 2H); HRMS (CI, CH_4) exact mass calcd for $C_{50}H_{57}F_2N_4O_{10}$ 911.4042 (MH^+), found 911.4060. Anal. Calcd for $C_{50}H_{56}F_2N_4O_{10}$: C, 65.92; H, 6.20; N, 6.15. Found: C, 66.15; H, 6.01; N, 6.20.

5,15-[Bis(4-fluorophenyl)]-10,20-diethylporphyrin (15). From 1,1-dipyrrylpropane and 4-fluorobenzaldehyde in 16% yield: red-brown powder; R_f 0.71 (99.7:0.3 $CHCl_3$/MeOH); UV-vis ($CHCl_3$) λ_{max} 401 nm (ϵ = 49 000 cm^{-1} M^{-1}), 502 (ϵ = 8100), 535 (ϵ = 2807), 576 (ϵ = 2800), 630 (ϵ = 1017); ^1H NMR (400 MHz, $CDCl_3$) δ 9.32 (d, 4H), 9.11 (d, 4H), 8.22 (m, 4H), 7.50 (m, 4H), 2.85 (q, *J* = 6.3 Hz, 4H), 1.46 (t, *J* = 6.3 Hz, 6H), -3.13 (bs, 2H).Anal. Calcd for $C_{36}H_{28}F_2N_4$: C, 77.96; H, 5.09; N, 10.10. Found: C, 78.05; H, 4.93; N, 10.43.

Synthesis of Glycoporphyrins. Typical BF_3-Promoted Condensation Procedure: 5,15-[Bis(4-fluorophenyl)]-10α,20β- and 10α,20α-[bis(1,2,4-tri-*O*-benzyl-D-*arabino*-tetritol-1-yl)]-porphyrins (9 and 14). To a solution of dipyrrylmethane **5** (100 mg, 0.19 mmol) in 40 mL of CH_2Cl_2 were added sequentially 4-fluorobenzaldehyde (21 μL, 0.19 mmol) and BF_3 etherate (48 μL, 0.38 mmol) at 0 °C under an argon atmosphere. The reaction vessel was shielded from light while stirring was continued for 4.5 h. Triethylamine (53 μL, 0.38 mmol) and then DDQ (90.8 mg, 0.4 mmol) were added, and the mixture was stirred at room temperature for an additional 5 h. The solvent was evaporated, and the crude reaction products were worked up and purified as described above in the CF_3CO_2H-promoted procedure. There were obtained porphyrin **9** and porphyrin **14** in 6% and 4% yield, respectively. For **14**: dark-brown solid; R_f 0.56 (99.7:0.3 $CHCl_3$/MeOH); $[\alpha]^{20}_{589}$ -312.5° (*c* 0.003, $CHCl_3$); UV-vis ($CHCl_3$) λ_{max} 417 nm (ϵ = 27 420 cm^{-1} M^{-1}), 518 (ϵ = 2330), 547 (ϵ = 1395), 598 (ϵ = 830), 653 (ϵ = 3670); CD ($CHCl_3$) $[\theta]_{417}$ = -2390 deg cm^2 $dmol^{-1}$, $[\theta]_{518}$ = -765, $[\theta]_{548}$ = +591, $[\theta]_{598}$ = -63, $[\theta]_{653}$ = -2550; ^1H NMR (600 MHz, $CDCl_3$) δ 10.04 (d, *J* = 5.1 Hz, 1H), 9.84 (d, *J* = 4.5 Hz, 1H), 9.79 (d, *J* = 5.1 Hz, 1H), 9.03 (d, *J* = 4.9 Hz, 1H), 8.49 (d, *J* = 5.1 Hz, 1H), 8.41 (d, *J* = 4.9 Hz, 1H), 8.34 (d, *J* = 4.5 Hz, 1H), 8.09 (d, *J* = 5.1 Hz, 1H), 7.90–7.60 (m, 4H), 7.40 (m, 4H), 7.35–6.50 (m, 30H), 7.30 (m, 1H), 6.30 (m, 1H), 4.72–4.50 (m, 5H), 4.42 (m, 1H), 4.28 (m, 7H), 4.18 (m, 2H), 3.90-3.40 (m, 7H), 2.62 (bs, 2H), -1.00 and -1.40 (2bs, 2H); HRMS (CI, CH_4) exact mass calcd for $C_{82}H_{73}F_2N_4O_8$ 1279.5396 (MH^+), found 1279.5415. Anal. Calcd for $C_{82}H_{72}F_2N_4O_8$: C, 76.98; H, 5.67; N, 4.38. Found: C, 77.21; H, 5.89; N, 4.20.

By using a similar experimental procedure the following porphyrin was also prepared.

5,15-[Bis(4-fluorophenyl)]-10α,20β-[bis(1,2-*O*-isopropylidene-3-*O*-methyl-β-L-threofuranos-4-yl)porphyrin (13). From dipyrrylmethane **8** and 4-fluorobenzaldehyde: yield 3.6%; a brown glassy solid; R_f 0.62 (99.7:0.3 $CHCl_3$/MeOH); $[\alpha]^{20}_{546}$ -41.7°, $[\alpha]^{20}_{589}$ -50.0° (*c* 0.01, $CHCl_3$); UV-vis ($CHCl_3$) λ_{max} 421 nm (ϵ = 13 260 cm^{-1} M^{-1}), 517 (ϵ = 555), 553 (ϵ = 477), 591 (ϵ = 380), 645 (ϵ = 190); CD ($CHCl_3$) $[\theta]_{421}$ = -4625 deg cm^2 $dmol^{-1}$, $[\theta]_{517}$ = -21, $[\theta]_{553}$ = -21, $[\theta]_{591}$ = -21, $[\theta]_{645}$ = -28; ^1H NMR δ 9.62 (d, *J* = 5.1 Hz, 2H), 8.81 (m, 2H), 8.73 (d, *J* = 5.1 Hz, 3H), 8.10 (m, 4H), 7.83 (m, 1H), 7.38 (m, 4H), 7.30 (m, 2H), 6.63 (m, 2H), 5.20 (m, 6H), 4.25 (m, 2H), 3.96 (m, 2H), 1.32 (s, 6H), 1.20 (s, 6H), -2.90 (bs, 2H); HRMS (CI, CH_4) exact mass calcd for $C_{48}H_{45}F_2N_4O_8$ 843.3205 (MH^+), found 843.3219. Anal. Calcd for $C_{48}H_{44}F_2N_4O_8$: C, 68.40; H, 5.26; N, 6.65. Found: C, 68.68; H, 5.34; N, 6.51.

Computational Methods. Molecular mechanics calculations were performed on a Silicon Graphics 4D35GT workstation, running the Insight & Discover molecular modeling package (v. 2.2.0, Biosym Technologies, San Diego, CA). The force-field, chosen from the software library, was CVFF (reparameterized for heme rings and including contributions for bond stretching with the Morse equation) and was used without any further modification. Structures were generated using fragments of standard bond lengths and angles and energy minimized with a conjugate gradients algorithm, until the maximum derivative over any atomic coordinate was less then 0.1 kcal mol^{-1} $Å^{-2}$. To avoid local energy minima, the structure was subjected to a short molecular dynamics run of 300 ps at 300 K and further minimized. The inversion barrier of the carbohydrate side chains was calculated by forcing the torsional angles with a force equal to 100 kcal rad^{-2}, starting from -120° to +120° in steps of 20° each and subsequent energy minimization.

Acknowledgment. This work was supported by the Consiglio Nazionale delle Ricerche, Progetto Finalizzato Chimica Fine. The authors acknowledge the Centro Interfacoltà di Misure dell'Università di Parma for instrumental facilities. We are also grateful for helpful discussions with Prof. Lucio Merlini.